Received: 4 March 2020 | Revised: 23 June 2020 | Accepted: 24 June 2020

DOI: 10.1111/ffe.13296



ORIGINAL CONTRIBUTION

FFEMS Fatigue & Fracture of Engineering Materials & Structures

WILEY

# Fatigue life prediction of woven composite laminates with initial delamination

**Aoshuang Wan**[1] | **Junjiang Xiong**[1] | **Yigeng Xu**[2]

[1]School of Transportation Science and Engineering, Beihang University, Beijing, 100191, China

[2]School of Aerospace, Transport and Manufacturing, Cranfield University, Cranfield, MK43 0AL, UK

**Correspondence**
Yigeng Xu, School of Aerospace, Transport and Manufacturing, Cranfield University, Cranfield MK43 0AL, UK.
Email: yigeng.xu@cranfield.ac.uk

**Funding information**
National Natural Science Foundation of China, Grant/Award Numbers: 51375033, 51875021

**Abstract**

An engineering approach for fatigue life prediction of fibre-reinforced polymer composite materials is highly desirable for industries due to the complexity in damage mechanisms and their interactions. This paper presents a fatigue-driven residual strength model considering the effect of initial delamination size and stress ratio. Static and constant amplitude fatigue tests of woven composite specimens with delamination diameters of 0, 4 and 6 mm were carried out to determine the model parameters. Good agreement with experimental results has been achieved when the modified residual strength model has been applied for fatigue life prediction of the woven composite laminate with an initial delamination diameter of 8 mm under constant amplitude load and block fatigue load. It has been demonstrated that the residual strength degradation-based model can effectively reflect the load sequence effect on fatigue damage and hence provide more accurate fatigue life prediction than the traditional linear damage accumulation models.

**KEYWORDS**

delamination, fatigue life prediction, residual strength, woven composite laminate

## 1 | INTRODUCTION

Woven composite laminates demonstrate good combined shear strength and impact resistance and hence are widely used in transport and renewable energy industries.[1] Lack of reinforcement in the thickness direction is however a major concern for laminated composite components as it facilitates delamination under the influence of manufacture imperfections, low velocity impacts[2,3] and embedded active sensors.[4] Delamination poses a direct threat to the load-carrying capacity and residual service life of laminated composite components and is a major failure mode attracting serious attention. It has been reported that the compressive strength and subsequent failure modes are affected by the delamination shape (across-the-width straight line front, circular or peanut shaped),[5] size,[6,7] number[2] and through-thickness distribution.[8] The laminate failure caused by the buckling and delamination under static compressive load is also dependent on the length–width ratio of delamination.[9] The composite laminates with low length–width ratio delamination tends to kink, whereas high length–width ratio counterparts are prone to split under compression.[10] The fatigue behaviour of laminated composite structures is also influenced by the initial delamination.[11,12] Preexisting delamination has been linked to the change in failure mode during fatigue tests. It provides a prior path for layer separation, which then

propagates and spreads the damage to other layers until the final failure.[13] Lifshitz and Gildin[14] however reported that the preembedded delamination reduced the life of the specimen only when the delamination was located within a critical distance to the outer surface of the specimen. Reis et al.[15] found that artificial interlayer delamination had negligible influence on the tensile fatigue strength but reduced the strength significantly under fully reversed fatigue load. In addition, the voids at laminar interface also have a detrimental effect on the fatigue life of composite laminates. The crack measurement and fractographic analysis reveal that the effect of voids on the failure mechanisms is different for tension–tension and compression–compression loading conditions.[16]

Fatigue of composite materials involves complex interactive damage mechanisms of matrix cracking, fibre/matrix debonding, delamination and fibre breakage. It depends on many factors including lay-up configurations, fibre volume fraction, curing parameters, interfacial properties and loading and constraint conditions,[17] making it difficult to develop a satisfactory physical fatigue damage model that can account for all these factors and complicated interacting damage mechanisms for composite laminates. Instead, cumulative damage models could provide practical and efficient quantification of the fatigue damage accumulation in composites by relating macromechanical properties of composite components to the loading conditions. A significant body of investigation has been carried out to test the validity of Palmgren–Miner rule using different damage accumulation metrics for composite materials under variable amplitude loading. It was found that the linear Palmgren–Miner model does not work well for estimating accumulated damage of composite materials. The modified nonlinear Miner rules provided good life predictions for some composite components under spectrum loading[18–20] but did not work well for others.[21,22] Nevertheless, residual strength models seem to offer an effective engineering approach for life prediction under variable amplitude fatigue loads by relating directly the applied fatigue stress to the residual strength of the composite components.[23] It has been proven that using residual strength as damage metric could lead to better life prediction compared with the Palmgren–Miner damage rule.[24–26] Post et al.[27] pointed out that even the simple linear residual strength rule (Broutman and Sahu model[28]) could gain in accuracy of fatigue life prediction. Moreover, it was found that the damage accumulation evaluated by the residual strength model is nonlinear. Results in literature[29] show that cumulative fatigue damage under high–low block loading is different to that under low–high block loading, demonstrating that the residual strength model is capable of taking the load sequence effect into account in fatigue life prediction. Eskandari and Kim[30,31] developed a new nonlinear fatigue damage model associated with the SN curve that can predict the fatigue life and residual strength of composite materials. The fatigue lives of E-glass/epoxy composite material were predicted under a sequence load of two stress levels with the model, showing good agreement with the experimental results. Guedes[32] found that the Eskandari and Kim (E-K) model was valid for life predictions of woven E-glass fibre composite material under ascending and descending spectrum load but was invalid under fully random spectrum load. The E-K model was further modified by imposing a small decrease on model exponent when the peak stress increases, which improved the agreement with experimental results under different spectrum loads.

It is found from the literature review that limited amount of research on fatigue performance of composite materials has been focusing on the influence of delamination on constant amplitude fatigue behaviour and life prediction of unidirectional composite laminates under variable amplitude loading. The damage mechanisms of woven ply laminates are extremely difficult to separate and investigate due to complex microstructures resulting from the interlacing and undulating fibre tows. Little quantitative results can be found in literature for fatigue life prediction of woven composite laminates, particularly for the woven laminate with initial delamination and under spectrum loading. This paper aims at filling the gap by predicting the fatigue life of woven composite laminates with initial delamination under constant and variable amplitude loading using a modified residual strength model based on the authors' previous research.[33,34]

## 2 | DEVELOPMENT OF THE MODIFIED FATIGUE-DRIVEN RESIDUAL STRENGTH MODEL

### 2.1 | Model modification to account for the effect of initial delamination size

The change in residual strength of the woven composite laminates has been used as the fatigue damage variable in the author's original residual strength model.[33] The following relation has been proposed to correlate the number of fatigue cycles to the residual strength at a specific stress ratio of $r_0$:

$$n = C(s - S_0)^m [R_0 - R(n)]^b, \tag{1}$$

where $s$ is the maximum fatigue stress for tension–tension loading and is the absolute value of minimum

fatigue stress for compression–compression loading, $R(n)$ is the residual strength of the composite material, $n$ is the number of fatigue cycles, $S_0$ is the fatigue limit of the pristine composite material, $R_0$ is the static strength of the pristine composite material and $C$, $m$ and $b$ are model parameters. $s$, $S_0$, $R_0$ and $R(n)$ are of the unit of MPa. As the residual strength $R(n)$ decreases with the increase of fatigue stress $s$ and fatigue cycles $n$, model parameter $m$ is normally negative whereas $b$ is positive to characterize the relation among residual strength, fatigue stress and fatigue cycles. The residual strength model (Equation 1) is a phenomenological model to characterize strength degradation of composite materials under fatigue load, which allows dimensional inconsistency between residual strength (or fatigue stress) and fatigue cycles. A good agreement was achieved between the predictions and the actual experimental results when the undamaged woven laminate was under constant amplitude fatigue loading.[33]

The residual strength model (Equation 1) was developed for laminates with double edge notches to account for the notch effect on residual strength.[34] Note that the residual strength model in Wan et al.[34] is a phenomenological model characterizing the fatigue damage accumulation by using strength degradation instead of physical damage. Because the initial delamination damage also has a detrimental effect on residual strength and fatigue life similar to the notch damage,[5–15] the residual strength model in literature[34] has been modified for the laminate with a central circular delamination in this paper. It is also worth noting that only the effect of damage size on residual strength and fatigue life was considered in literature.[34] A further modification is introduced in this paper by normalizing the initial damage size with the laminate width to reflect the effect of damage size more accurately.

The following relations are presented to relate the static and fatigue strengths of pristine woven laminate to those of damaged laminate with an initial circular delamination at the centre of the midplane:

$$R_0 = R_0^0\left(1-\alpha_1 k^{\beta_1}\right), \tag{2}$$

$$S_0 = S_0^0\left(1-\alpha_2 k^{\beta_2}\right), \tag{3}$$

where $k=\frac{d}{w}$, $d$ is the initial damage size (diameter of the initial circular delamination), $w$ is the width of the specimen and $R_0$ and $S_0$ are the static and fatigue strengths of the composites with an initial delamination of diameter–width ratio $k$. By using the experimental data on residual strengths of composite laminates with midplane circular delamination in literatures,[7,9] the relationship between $R_0$ and $k$ (Equation 2) is fitted and plotted in Figure 1. Note that Figure 1A illustrates the fitting curve from residual strength data of T300/QY8911 composite laminates with the lay-up of $[(45/0/-45/90)_3/45/0//-45/90/(90/-45/0/45)_4]$ where the symbol "//" represents the position of initial circular delamination.[9] Figure 1B illustrates the fitting curves from residual strength data of three types of T300/QY8911 composite laminates with midplane initial circular delamination which have three different stacking sequences (Type A: $[45/-45/0/-45/0/45/90/0/45/90/-45/0]_s$, Type B: $[45/-45/0/-45/0/45/0/-45/45/45/90/45/-45/-45/45/0]_s$, Type C: $[45/-45/0/-45/0/45/90/-45/0/45/90/45/0/-45/90/0]_s$).[7] Good agreement between experimental data and fitting curves has been achieved, demonstrating the validity of above mathematical assumptions.

Substituting Equations 2 and 3 into Equation 1 shows

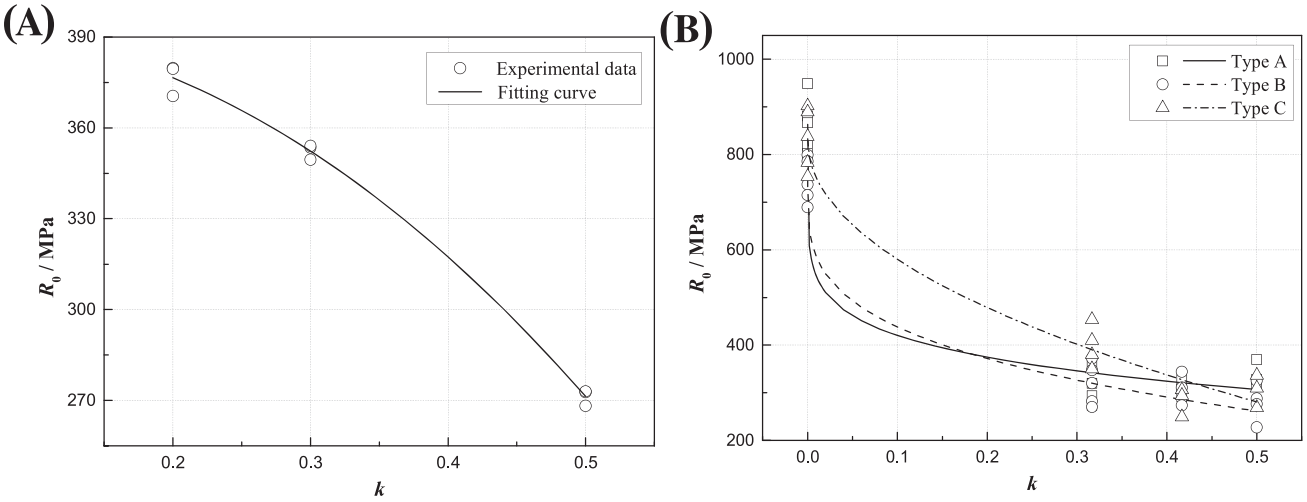


**FIGURE 1** Variation of static strength $R_0$ with diameter–width ratio $k$: (A) experimental data from literature,[9] (B) experimental data from literature[7]

$$n = C\left[s - S_0^0\left(1-\alpha_2 k^{\beta_2}\right)\right]^m \left[R_0^0\left(1-\alpha_1 k^{\beta_1}\right) - R(n)\right]^b. \quad (4)$$

Equation 4 is the governing equation of the residual strength model accounting for the effect of normalized delamination size. The initial residual strength of the delaminated composite component is usually obtained from the static test, and the model constants $\alpha_1$, $\beta_1$ and $R_0^0$ are obtained from the static test data by means of the linear regression principle. The residual strength data of fatigue tests are used to determine the model parameters $\alpha_2$, $\beta_2$, $S_0^0$, $C$, $m$ and $b$ with the best fitting method.[34]

## 2.2 | Flowchart for life prediction with the residual strength degradation-based model

With the modified residual strength model shown in Equation 4, fatigue life can be determined through a cycle-by-cycle analysis based on the fatigue stress cycle and fatigue-driven degraded residual strength of the material. For a woven composite laminate with an initial delamination of diameter–width ratio $k$, the modified residual stress $s - n - R - k$ model shown in Equation 4 can be reduced to the form of $s - n - R$ residual strength surface model (Equation 1). The residual strength surface model at $n$ and $n+\Delta n$ loading cycles can be obtained as

$$\begin{cases} n = C(s-S_0)^m [R_0 - R(n)]^b \\ n+\Delta n = C(s-S_0)^m [R_0 - R(n+\Delta n)]^b \end{cases}. \quad (5)$$

Taking transformation of Equation 5 by subtraction gives

$$\Delta n = C(s-S_0)^m \left\{ [R_0 - R(n+\Delta n)]^b - [R_0 - R(n)]^b \right\}. \quad (6)$$

Rearranging Equation 6, the residual strength after $\Delta n$ number of loading cycles under constant amplitude fatigue stress $s$ can be obtained as

$$R(n+\Delta n) = R_0 - \left\{ \frac{\Delta n}{C(s-S_0)^m} + [R_0 - R(n)]^b \right\}^{\frac{1}{b}}. \quad (7)$$

Equation 7 is the iterative formula for residual strength of composites under fatigue load, which is a function of both the fatigue stress $s$ and the loading cycles $\Delta n$. Figure 2 shows the flowchart of the life prediction

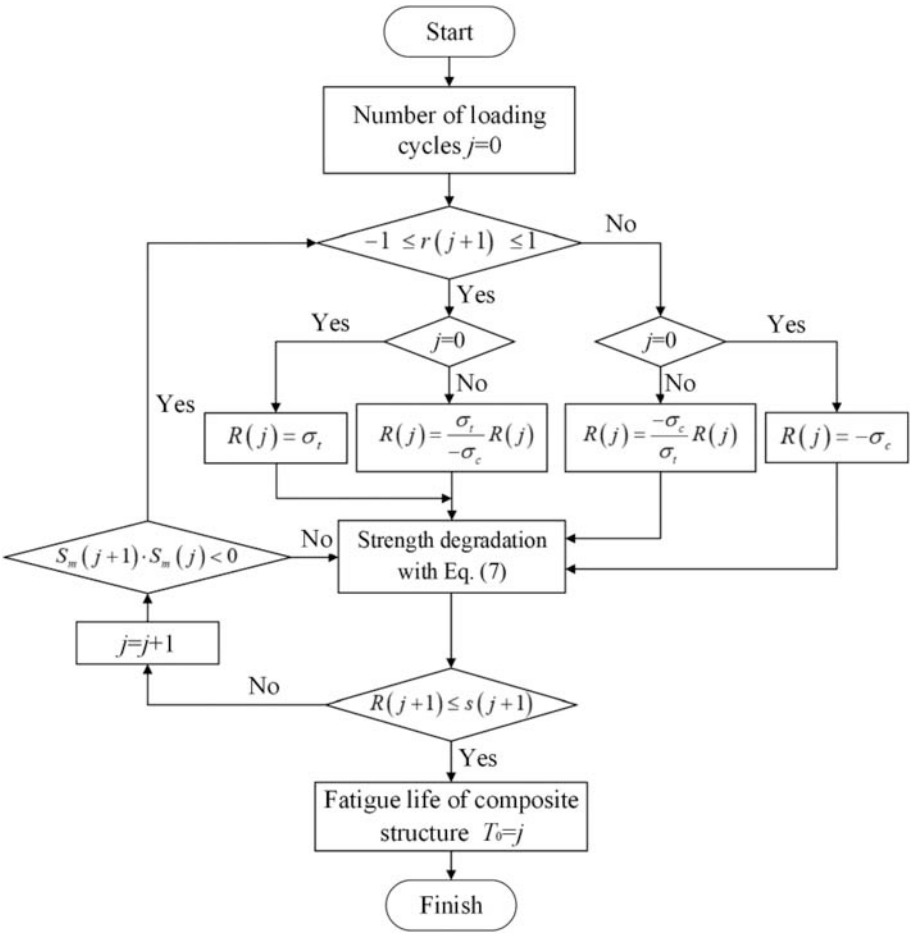


**FIGURE 2** Flowchart for residual strength degradation-based life prediction

procedure of the residual strength degradation-based model under variable amplitude fatigue loading. Note that in Figure 2, $r$ represents stress ratio of fatigue cycle, $S_m$ represents mean stress, $\sigma_t$ represents tensile strength and $\sigma_c$ represents compressive strength. The residual strength degradation of composites is calculated in a cycle-by-cycle manner using Equation 7. The model parameters in strength degradation formula (Equation 7) for composite materials at different stress ratios $r$ for fatigue life prediction under spectrum load will be derived in Section 3.3. In order to characterize the difference in tensile strength and compressive strength of the woven composite material, the ratio between tensile strength and compressive strength is used to adjust the residual strength of the material when transition between tension-dominated and compression-dominated fatigue cycles occurs. The final fatigue life is reached when the residual strength descends to be equal or less than the applied maximum stress of the fatigue cycle.

## 3 | RESULTS

### 3.1 | Results of static and fatigue tests and model parameters

Static and constant amplitude fatigue tests were carried out with Instron-8803 testing machine on two kinds of woven composite laminates (carbon fibre-reinforced polymer [CFRP] of 3238A/CF3052 and graphite fibre-reinforced polymer [GFRP] of 3238A/EW250F) with the lay-up of $[(45/-45)/(0/90)]_{3s}$. The specimen geometry is presented in Figure 3. Note that 'x' in Figure 3 is the delamination diameter that equals to 4, 6 or 8 mm for the delaminated specimens with the diameter–width ratio $k$ of $\frac{1}{9}$, $\frac{1}{6}$ and $\frac{2}{9}$, respectively. The circular delamination was introduced by inserting a Teflon film at the centre of the midplane of the specimen at the layup stage. The laminate plates were cured in an autoclave under 130°C curing temperature and 0.5-MPa pressure. Both the undamaged and delaminated plates were cut by a water jet.

As there is no standard test method for composite laminates with initial delamination, the open-hole static and fatigue test standards for composite laminates[35,36] were used for specimen design and testing in the current study. Following ASTM standards,[35,36] the static tests were performed under the loading rate of 2 mm/min. Following ASTM standard,[35] the constant amplitude fatigue tests were carried out under tension–tension at the stress ratio of 0.05 and under compression–compression at the stress ratio of 10 with the sinusoidal waveform at frequency of 10 Hz. Figure 4 shows the test set-up where antibuckling device was used for the compressive static and fatigue tests. The antibuckling device was narrower than the specimens by 2 mm in order to

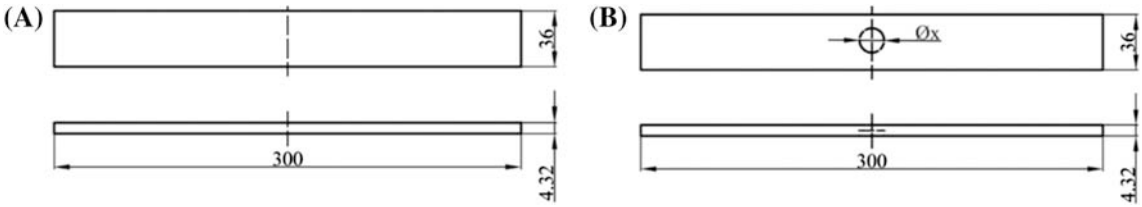


**FIGURE 3** Specimen: (A) without damage, (B) with initial delamination

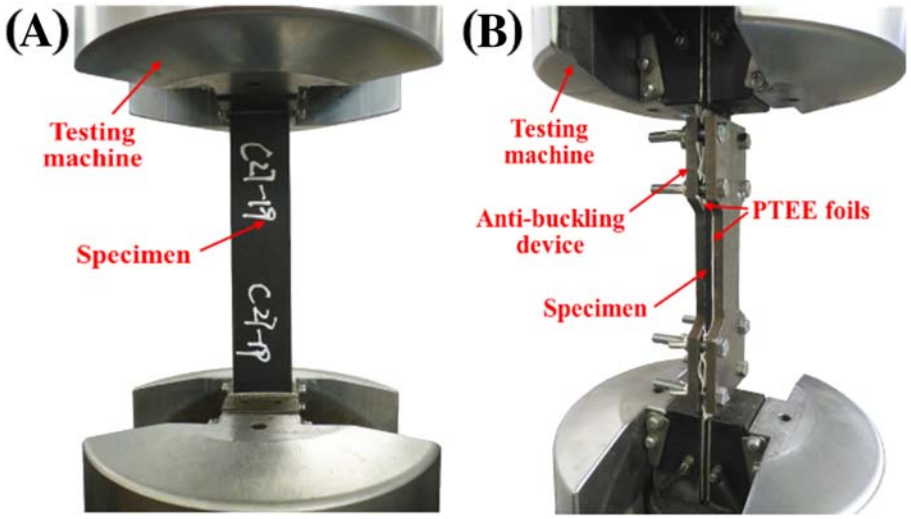


**FIGURE 4** Experiment assembly: (A) tensile static test and tension–tension fatigue test, (B) compressive static test and compression–compression fatigue test [Colour figure can be viewed at wileyonlinelibrary.com]

expose both unloaded edges of specimen with a clearance of 1 mm. Two antifriction polytetrafluoroethylene (PTEE) foils with the same dimensions as antibuckling device were placed between the specimen and the antibuckling device as shown in Figure 4.[37] The gap between specimen and the antibuckling fixture was checked by using a feeler gage (0.05 ± 0.05 mm) after installation to ensure no bending contributes to compression.[36] For each type of specimen, four applied stress levels were chosen to achieve fatigue lives of $10^4$, $10^5$, $5 \times 10^5$ and $10^6$ cycles. Five specimens were employed under each applied stress level. If the specimen survived at the target fatigue life, it was tested up to failure according to the static test standard[35,36] to determine the residual strength.

Figure 5 presents the failed specimens during tensile and compressive fatigue tests. It can be seen from Figure 5 that the fatigue specimens under tensile fatigue load show fibre-dominated failure modes whereas those under compressive fatigue load are controlled by matrix-dominated failure modes. The damage initiates from the circular delamination and propagates until final failure of the specimens. The presence of internal artificial delamination offers a preferential way for interlayer delamination under tensile fatigue loading (shown in Figure 5A), which leads to the disruption of the effective stress transfer between layers. Massive breakage and pull-out of fibres subsequently happen to cause the final fracture of specimen. On the other hand, the damage initiates from the embedded delamination and final failure happens at the location of delamination under compressive fatigue loading as stress concentration and local buckling exists near the embedded delamination (shown in Figure 5B). The specimens under static loading show similar failure modes to specimens under fatigue loading as shown in Figure 5.

The static strengths of undamaged and delaminated woven GFRP and CFRP composites are presented in Table 1, which are calculated on the basis of the gross cross-sectional area of the specimen. It can be seen from Table 1 that the coefficients of variation for the static strength results are less than 5%, indicating that the scatter of the test results is acceptable. In addition, analysis of variance has been performed to determine the significance of differences for static strength results (tensile/compressive strengths of GFRP/CFRP composites) in Table 1. It shows that the significance levels of differences for static strength results in Table 1 are below 0.01. Thus, it can be concluded from Table 1 that the tensile and compressive strengths of woven composites decrease with the increase in delamination diameter, indicating that the initial delamination has a detrimental effect on static strength. The detrimental effect is stronger in compression as the percentage reduction in compressive strength is greater than that in tension for both materials.

The fatigue experimental data of woven GFRP and CFRP composites are plotted in Figure 6. It is worth noting that the data points marked with arrows and residual strength values in brackets represent the survival specimens that were tested under static loading after the targeted fatigue life. The effect of delamination is again greater under compressive fatigue load than under tensile fatigue load, which is consistent with the effect of delamination on static strength. The residual strength of the fatigued composite laminate is lower than the initial strength listed in Table 1. There is however no direct correlation among the residual strengths of the run-out specimens at target fatigue lives of $10^5$, $5 \times 10^5$ and $10^6$ cycles. This is expected as these run-out samples were tested under different fatigue stress levels in order to achieve different target fatigue lives. The fatigue damage accumulation after the targeted fatigue life of $10^6$ cycles could be

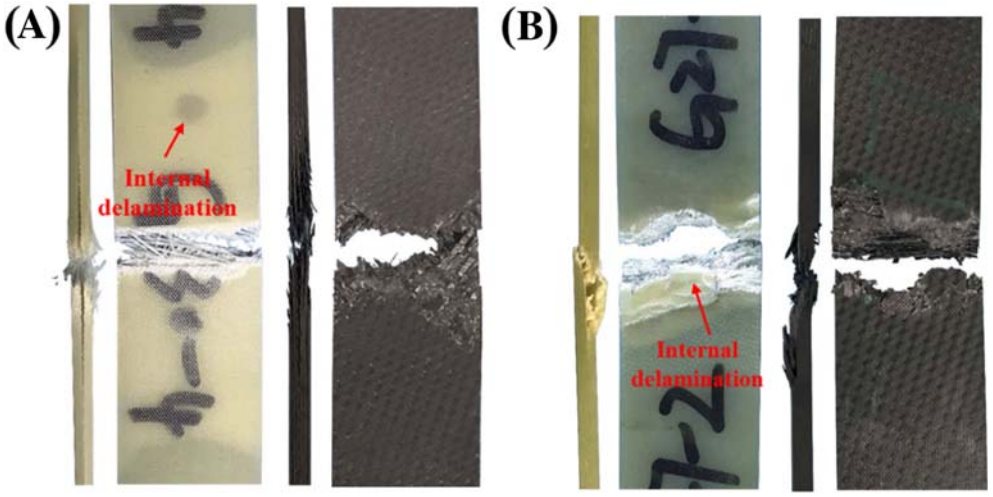


**FIGURE 5** Failed specimens: (A) under tensile fatigue loading, (B) under compressive fatigue loading [Colour figure can be viewed at wileyonlinelibrary.com]

**TABLE 1** Results of static strength (unit: MPa)

| Composites | Loading direction | Data | 0 | 4 mm | 6 mm | 8 mm |
|---|---|---|---|---|---|---|
| GFRP | Tension | Test results | 346.8, 355.1, 358.9, 342.1, 344.4 | 329.0, 348.4, 331.6, 323.2, 343.7 | 323.2, 331.3, 341.8, 330.5, 328.7 | 315.1, 330.2, 331.9, 328.0, 333.8 |
| | | Mean value | 349.5 | 335.2 | 331.1 | 327.8 |
| | | Standard deviation | 7.21 | 10.51 | 6.76 | 7.41 |
| | | Coefficient of variation | 2.1% | 3.1% | 2.0% | 2.3% |
| | Compression | Test results | 225.1, 237.7, 239.7, 234.6, 240.9 | 223.3, 220.8, 222.4, 209.3, 216.3 | 207.2, 220.0, 212.0, 213.9, 222.1 | 218.8, 212.4, 214.5, 209.2, 211.2 |
| | | Mean value | 235.6 | 218.4 | 215.0 | 213.2 |
| | | Standard deviation | 6.34 | 5.77 | 6.05 | 3.66 |
| | | Coefficient of variation | 2.7% | 2.6% | 2.8% | 1.7% |
| CFRP | Tension | Test results | 552.1, 547.3, 538.9, 532.0, 538.7 | 487.0, 473.4, 452.9, 466.6, 481.1 | 478.1, 467.2, 461.3, 448.3, 463.5 | 464.3, 468.5, 459.2, 459.6, 443.8 |
| | | Mean value | 541.8 | 472.2 | 463.7 | 459.1 |
| | | Standard deviation | 7.91 | 13.26 | 10.75 | 9.35 |
| | | Coefficient of variation | 1.5% | 2.8% | 2.3% | 2.0% |
| | Compression | Test results | 409.4, 424.8, 421.8, 419.7, 412.5 | 341.9, 351.4, 355.8, 331.1, 342.9 | 327.7, 346.2, 342.6, 326.0, 339.1 | 340.2, 339.0, 321.4, 332.3, 323.9 |
| | | Mean value | 417.6 | 344.6 | 336.3 | 331.3 |
| | | Standard deviation | 6.46 | 9.54 | 9.02 | 8.55 |
| | | Coefficient of variation | 1.5% | 2.8% | 2.7% | 2.6% |

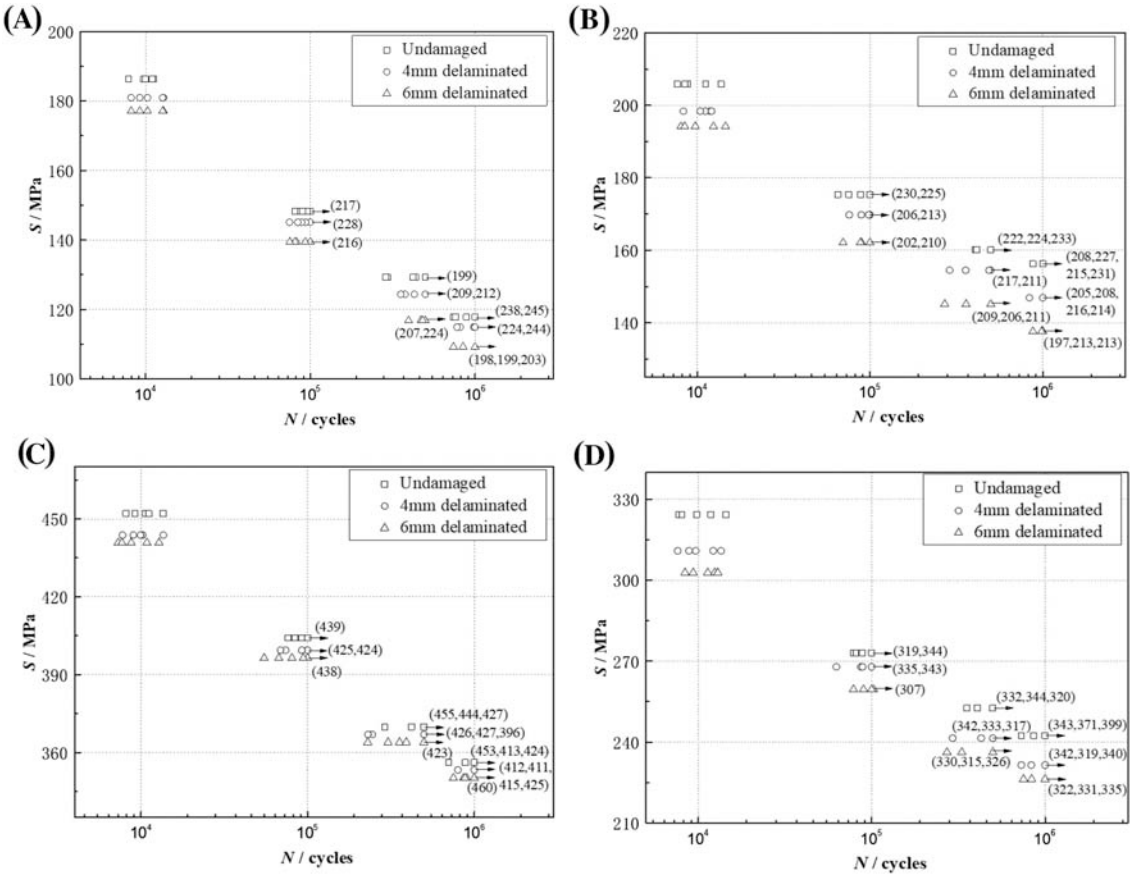


**FIGURE 6** Tension–tension and compression–compression fatigue test results: (A) woven graphite fibre-reinforced polymer (GFRP) under tension–tension loading, (B) woven GFRP under compression–compression loading, (C) woven carbon fibre-reinforced polymer (CFRP) under tension–tension loading, (D) woven CFRP under compression–compression loading (unit: MPa)

smaller than the damage after the targeted fatigue life of $5 \times 10^5$ cycles as the applied fatigue stress to achieve $10^6$ target life is lower than the stress to achieve $5 \times 10^5$ cycles.

Test results in Table 1 and Figure 6 have been used to determine the model parameters and confidence intervals by following the method in Wan et al.[34] Taking the logarithm form of Equation 4 gives

$$y = a_0 + a_1 x_1 + a_2 x_2, \tag{8}$$

where

$$y = \lg n, \tag{9}$$

$$x_1 = \lg\left[s - S_0^0\left(1 - \alpha_2 k^{\beta_2}\right)\right], \tag{10}$$

$$x_2 = \lg\left[R_0^0\left(1 - \alpha_1 k^{\beta_1}\right) - R(n)\right], \tag{11}$$

$$a_0 = \lg C, \tag{12}$$

$$a_1 = m, \tag{13}$$

$$a_2 = b. \tag{14}$$

By using the experimental data $(s_i, n_i, R_i, k_i)$ $(i = 1,2,\cdots,l)$ and binary linear regression method based on the minimum value principle of residual sum of squares $Q\left(S_0^0, \alpha_2, \beta_2\right)$, the estimated value of $a$ can be obtained as

$$\hat{a} = (X'X)^{-1}X'Y, \tag{15}$$

where

$$\hat{a} = \begin{bmatrix} \hat{a}_0 \\ \hat{a}_1 \\ \hat{a}_2 \end{bmatrix}, \tag{16}$$

$$X = \begin{bmatrix} 1 & x_{11} & x_{21} \\ 1 & x_{12} & x_{22} \\ \vdots & \vdots & \vdots \\ 1 & x_{1l} & x_{2l} \end{bmatrix}, \tag{17}$$

$$Y = \begin{bmatrix} y_1 \\ y_2 \\ \vdots \\ y_l \end{bmatrix}. \tag{18}$$

The 95% confidence lower and upper limits are determined as[38]

$$n = C\left[s - S_0^0\left(1-\alpha_2 k^{\beta_2}\right)\right]^m \left[R_0^0\left(1-\alpha_1 k^{\beta_1}\right) - R(n)\right]^b 10^{-\delta(k,s,R)}, \tag{19}$$

$$n = C\left[s - S_0^0\left(1-\alpha_2 k^{\beta_2}\right)\right]^m \left[R_0^0\left(1-\alpha_1 k^{\beta_1}\right) - R(n)\right]^b 10^{\delta(k,s,R)}, \tag{20}$$

with

$$\delta(k,s,R) = t_{0.975}(l-3)\cdot\sqrt{\frac{Q}{l-3}}\cdot\sqrt{1+x(X'X)^{-1}x'}, \tag{21}$$

$$x = [1\ x_1\ x_2], \tag{22}$$

$$Q = \sum_{i=1}^{l}\left(y_i - \hat{a}_0 - \hat{a}_1 x_{1i} - \hat{a}_2 x_{2i}\right)^2, \tag{23}$$

where $Q$ is the residual sum of squares. $\delta$ is the confidence interval function with respect to $k$, $s$ and $R$.

Table 2 lists the determined model parameters of $s-n-R-k$ residual strength models for woven GFRP and CFRP composites. As binary linear regression analysis was applied to estimate the model parameters, square of the correlation coefficient $R^2$ is also listed in Table 2. In addition, the significance levels of the regression coefficients (i.e., estimated model parameters $m$ and $b$ in Table 2) are below 0.01.

## 3.2 | Fatigue life prediction under constant amplitude loading

The model parameters in Table 2 are employed for fatigue life prediction of specimens with 8-mm initial delamination ($k=\frac{2}{9}$) under constant amplitude loading. By substituting the given diameter–width ratio of the delamination ($k=\frac{2}{9}$) to the $s-n-R-k$ model, Equation 4 becomes the $s-n-R$ residual strength surface models for woven GFRP and CFRP composites with 8-mm initial delamination. The $s-n-R$ surface models are further reduced to the SN fatigue curve models plotted in Figure 7 by making $s=R$ according to the residual strength criterion.

Figure 7 shows the comparison between the experimental result and model prediction of woven GFRP and CFRP with 8-mm initial delamination at stress ratios of 0.05 and 10. The 95% confidence limits for the model prediction curves are also plotted in Figure 7. Unlike typical SN curves showing larger width of confidence intervals at the upper and bottom ends in comparison with the middle of the experimental data, the width of the confidence interval shows little variation for all four cases presented. This is due to the fact that the testing data of the current study cover only the middle part of the SN curve of this composite material, not including all three regimes of the fatigue data. The good correlation between the model prediction and experimental result demonstrates that the developed $s-n-R-k$ residual strength model is capable of predicting the fatigue life of delaminated woven laminate under constant amplitude fatigue loading.

## 3.3 | Fatigue life prediction under block loading

Figure 8 illustrates the load history of block loading fatigue tests including two-stage tests at the stress ratio of

**TABLE 2** Model parameters of modified residual strength models for woven laminates with central circular delamination

| Materials | Stress ratio | $\alpha_1$ | $\beta_1$ | $R_0^0$ (MPa) | $\alpha_2$ | $\beta_2$ | $S_0^0$ (MPa) | $C$ | $m$ | $b$ | $R^2$ |
|---|---|---|---|---|---|---|---|---|---|---|---|
| GFRP | 0.05 | 0.15 | 0.60 | 349.45 | 5.21 | 1.82 | 44.72 | $8.50\times10^{16}$ | −6.54 | 0.53 | 0.91 |
| | 10 | 0.19 | 0.44 | 235.60 | 6.04 | 2.10 | 119.28 | $2.36\times10^{13}$ | −4.89 | 0.12 | 0.93 |
| CFRP | 0.05 | 0.24 | 0.28 | 541.82 | 4.11 | 2.39 | 116.75 | $4.55\times10^{36}$ | −13.09 | 0.21 | 0.97 |
| | 10 | 0.31 | 0.27 | 417.63 | 3.20 | 2.07 | 166.73 | $9.07\times10^{15}$ | −5.74 | 0.36 | 0.91 |

Abbreviations: CFRP, carbon fibre-reinforced polymer; GFRP, graphite fibre-reinforced polymer.

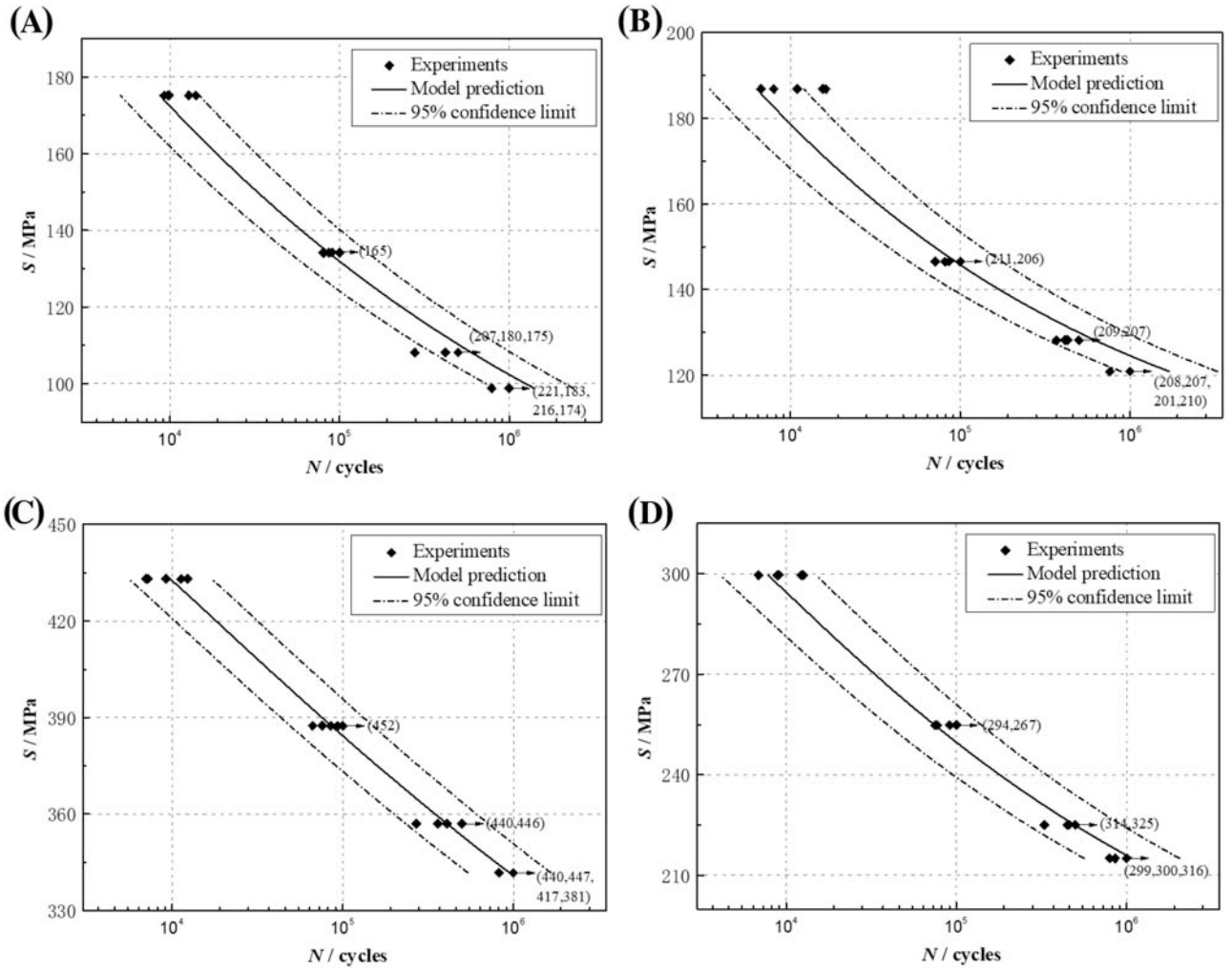


**FIGURE 7** Comparison between model predictions and constant amplitude fatigue experimental data of woven laminates with 8-mm initial delamination: (A) woven graphite fibre-reinforced polymer (GFRP) under tension–tension loading, (B) woven GFRP under compression–compression loading, (C) woven carbon fibre-reinforced polymer (CFRP) under tension–tension loading, (D) woven CFRP under compression–compression loading

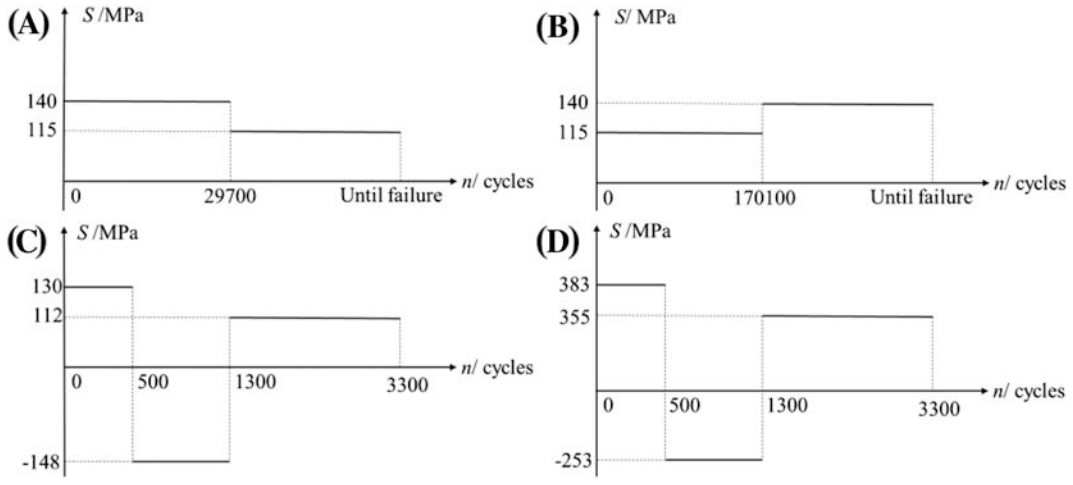


**FIGURE 8** Load history of block loading fatigue tests: (A) high–low two-stage test of woven graphite fibre-reinforced polymer (GFRP) composites, (B) low–high two-stage test of woven carbon fibre-reinforced polymer (CFRP) composites, (C) high–low–high repeated test of woven GFRP composites, (D) high–low–high repeated test of woven CFRP composites

0.05 (high–low and low–high sequences) and repeated block tests consisting of stress ratios of 0.05 and 10 (high–low–high sequence). Note that the stress ratio sequence for repeated high–low–high sequence is 0.05–10–0.05, and '*S*' in Figure 8 represents the absolute maximum fatigue stress of the fatigue cycle. The fatigue cycles of the first block of the two-stage fatigue tests (Figure 6A,B) account for 50% of the theoretical fatigue life corresponding to the applied stress level. The load spectrum of the high–low–high sequence in Figure 6C,D was repeated until the failure of the material. A minimum of three specimens were tested under each type of block load.

The model parameters in Table 2 are employed for fatigue life prediction of specimens with 8-mm initial delamination ($k=\frac{2}{9}$) under block loading. Equation 4 is the residual strength model accounting for the effect of normalized delamination size at a specific stress ratio $r_0$. Note that $r_0$ is the stress ratio at which the experimental data and model parameters have been determined (such as 0.05 or 10 as shown in Table 2). However, actual engineering structures often suffer from variable amplitude spectrum load under different stress ratios as shown in Figure 8. Although the load history in Figure 8 only consists of stress ratios 0.05 and 10, there exists a large number of actual spectrum load history that contain different stress ratios without known test data and model parameters. It is therefore important to extend the determined residual strength model at a specific stress ratio $r_0$ to be suitable for arbitrary stress ratio $r$. The modified Goodman diagram shown in Figure 9 is adopted to modify Equation 4 to account for the effect of stress ratio on fatigue life[34]:

$$\frac{S_a}{S_{-1}}+\frac{S_m}{\sigma_b}=1, \tag{24}$$

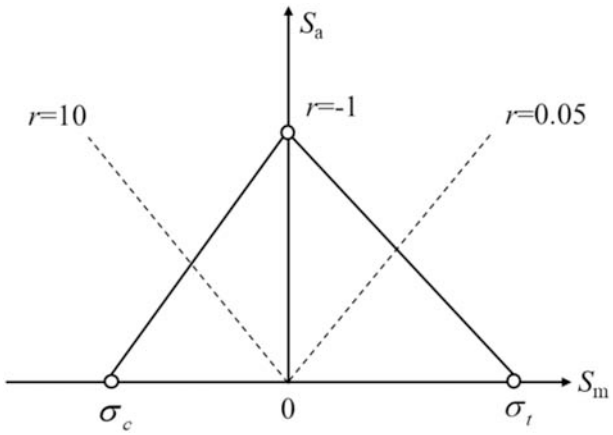


**FIGURE 9** Constant life diagram considering the effect of compressive mean stress[34]

where $S_a$ and $S_m$ are the stress amplitude and mean stress of the fatigue cycle, $S_{-1}$ is the fatigue endurance limit under fully reversed cyclic loading and $\sigma_b$ is the ultimate strength of the material that is either the ultimate tensile strength $\sigma_t$ when the absolute maximum fatigue stress is tensile ($-1 \le r \le 1$) or the ultimate compressive strength $\sigma_c$ when the absolute maximum fatigue stress is compressive ($r < -1$ or $r > 1$).

For a fatigue cycle of stress ratio $r$, it can be shown that

$$\begin{cases} S_a=\dfrac{1-r}{2}S_{\max,r} \\ S_m=\dfrac{1+r}{2}S_{\max,r} \end{cases}, \tag{25}$$

where $S_{\max,r}$ is the maximum fatigue stress at the stress ratio of $r$.

Substituting Equation 25 into Equation 24 shows

$$\frac{(1-r)S_{\max,r}}{2S_{-1}}+\frac{(1+r)S_{\max,r}}{2\sigma_t}=1. \tag{26}$$

At a given stress ratio $r_0$, Equation 26 becomes

$$\frac{(1-r_0)S_{\max,r_0}}{2S_{-1}}+\frac{(1+r_0)S_{\max,r_0}}{2\sigma_t}=1. \tag{27}$$

Taking transformation of Equations 26 and 27 to eliminate $S_{-1}$ yields

$$S_{\max,r_0}=\frac{2\sigma_b(1-r)}{(1-r_0)[2\sigma_b-(1+r)S_{\max,r}]+(1+r_0)(1-r)S_{\max,r}}S_{\max,r}. \tag{28}$$

Equation 28 gives the absolute maximum fatigue stress $s$ when $-1 \le r \le 1$, $-1 \le r_0 \le 1$ and $\sigma_b = R_0$ representing the initial tensile static strength of the laminate with initial delamination.

By means of the definition of the stress ratio, one has

$$\begin{cases} S_{\max,r}=S_{\min,r}/r \\ S_{\max,r_0}=S_{\min,r_0}/r_0 \end{cases}, \tag{29}$$

where $S_{\min,r}$ and $S_{\min,r_0}$ are the minimum fatigue stress.

Substituting Equation 29 into Equation 28 gives

$$|S_{\min,r_0}|=\frac{2\sigma_b r_0(1-r)}{(1-r_0)[2r\sigma_b+(1+r)|S_{\min,r}|]-(1+r_0)(1-r)|S_{\min,r}|}|S_{\min,r}|. \tag{30}$$

Equation 30 gives the absolute maximum fatigue stress $s$ when $r < -1$ or $r > 1$, $r_0 < -1$ or $r_0 > 1$ and $\sigma_b = -R_0$

representing the initial compressive static strength of the laminate with initial delamination.

Substituting Equations 28 and 30 into Equation 4 leads to Equation 31 is the modified fatigue-driven residual strength $s-n-R-k-r$ model that can quantitatively characterize the effect of delamination size and stress ratio on fatigue life and residual strength of the composite component.

$$\begin{cases} n = C\left\{\dfrac{2R_0^0\left(1-\alpha_1 k^{\beta_1}\right)(1-r)S_{\max,r}}{(1-r_0)\left[2R_0^0\left(1-\alpha_1 k^{\beta_1}\right)-(1+r)S_{\max,r}\right]+(1+r_0)(1-r)S_{\max,r}} \right. & \left(\begin{matrix}-1\le r\le 1,\\ -1\le r_0\le 1\end{matrix}\right), \\ \left. -S_0^0\left(1-\alpha_2 k^{\beta_2}\right)\right\}^m\left[R_0^0\left(1-\alpha_1 k^{\beta_1}\right)-R(n)\right]^b & \\ n = C\left\{\dfrac{-2r_0R_0^0\left(1-\alpha_1 k^{\beta_1}\right)(1-r)|S_{\min,r}|}{(1-r_0)\left[-2rR_0^0\left(1-\alpha_1 k^{\beta_1}\right)+(1+r)|S_{\min,r}|\right]-(1+r_0)(1-r)|S_{\min,r}|} \right. & \left(\begin{matrix}r<-1 \text{ or } r>1,\\ r_0<-1 \text{ or } r_0>1\end{matrix}\right). \\ \left. -S_0^0\left(1-\alpha_2 k^{\beta_2}\right)\right\}^m\left[R_0^0\left(1-\alpha_1 k^{\beta_1}\right)-R(n)\right]^b & \end{cases} \tag{31}$$

Both the linear Palmgren–Miner rule and the residual strength degradation-based model are used to predict the fatigue life for woven GFRP and CFRP composites with 8-mm initial delamination ($k=\frac{2}{9}$) under block loading. As mentioned earlier, substituting the given diameter–width ratio of the delamination and the stress ratio of fatigue cycle to the $s-n-R-k-r$ model leads to the $s-n-R$ residual strength surface model. Then according to the residual strength criterion, substituting $s=R$ into $s-n-R$ surface model leads to the SN fatigue curve models. By utilizing the Palmgren–Miner cumulative damage model with the SN curves, the fatigue life is predicted by accumulating the damage induced by each individual load block until the total damage of all the load blocks reaches a unit. For the life prediction using the residual strength degradation-based model, the $s-n-R$ surfaces are used to predict the degraded strength of woven GFRP and CFRP composites with 8-mm initial delamination during fatigue. The final fatigue life is obtained using the cycle-by-cycle analysis illustrated in the flowchart in Figure 2.

In addition, based on the SN fatigue curve models, the Hashin and Rotem model (Equation 32)[39] is also used to predict the fatigue life of woven GFRP and CFRP composites with 8-mm initial delamination. This model is nonlinear and has been applied in life prediction of composite materials (including woven composite materials) under spectrum load.[21,27]

$$D_i = D_{i-1}^{\frac{1-\sigma_i/\sigma_b}{1-\sigma_{i-1}/\sigma_b}} + \frac{n_i}{N_i}, \tag{31}$$

where $D_i$ and $D_{i-1}$ are the cumulative damage index for $i$th and $(i-1)$th block, respectively, $\sigma_i$ and $\sigma_{i-1}$ are the maximum absolute value of the fatigue stress for the $i$th and $(i-1)$th block, respectively, $\sigma_b$ is the ultimate strength of composite materials, which is either the ultimate tensile strength for tension-dominated loading or the ultimate compressive strength for compression-dominated loading, $n_i$ is the number of loading cycles for $i$th block and $N_i$ is the constant amplitude fatigue life at the stress level of $i$th block. Note that the cumulative damage index for the first block is $D_1 = n_1/N_1$.

Table 3 summarizes the experimental results and life predictions for woven GFRP and CFRP composites with 8-mm initial delamination under block fatigue load. It can be seen from the experimental results that the cumulative damage of woven composites follows the nonlinear damage accumulation rule. The fatigue life of woven GFRP composites under low–high sequence is shorter than Palmgren–Miner prediction but the fatigue life under high–low sequence is longer than Palmgren–Miner prediction, indicating that the loading sequence has great influence on fatigue damage accumulation of woven composites, which is consistent with literatures.[22,29] The fatigue lives predicted by Palmgren–Miner rule under low–high and high–low sequence are the same, indicating that the linear Palmgren–Miner model is not capable of taking the loading sequence effect into account. The fatigue life predicted by Hashin and Rotem model and the strength degradation-based model is shorter under low–high sequence than that under high–low sequence, showing the capacity of Hashin and Rotem model and the residual strength degradation-based model to account

**TABLE 3** The experimental results and life predictions of fatigue lives under block loading

| **Materials** | | **GFRP** | | | **CFRP** |
|---|---|---|---|---|---|
| **Loading** | | **High–low** | **Low–high** | **High–low–high** | **High–low–high** |
| Fatigue life (cycles, test results) | Test results | 227 199, 320 034, 285 996 | 176 427, 189 748, 176 881 | 112 912, 88 377, 179 336, 139 849, 138 802, | 135 639, 116 052, 130 700, 119 737, 105 923 |
| | Mean value | 277 743 | 181 018 | 131 855 | 121 610 |
| Fatigue life (cycles, Palmgren–Miner rule) | | 199 807 | 199 807 | 175 791 | 175 448 |
| Relative deviation to test results (%) | | 28 | 10 | 33 | 44 |
| Fatigue life (cycles, Hashin and Rotem model) | | 214 806 | 197 287 | 156 108 | 172 116 |
| Relative deviation to test results (%) | | 23 | 9 | 18 | 42 |
| Fatigue life (cycles, residual strength degradation) | | 210 713 | 197 773 | 99 692 | 151 800 |
| Relative deviation to test results (%) | | 24 | 9 | 24 | 25 |

Abbreviations: CFRP, carbon fibre-reinforced polymer; GFRP, graphite fibre-reinforced polymer.

for the loading sequence effect under block loading. The fatigue lives of woven composites under high–low–high sequence are shorter than Miner predictions for the two kinds of composites, demonstrating that the repetitive changes between tension–tension and compression–compression fatigue cycles can reduce the fatigue lives of woven composites, which is consistent with literature.[22]

The maximum relative deviations between fatigue life predictions and experiments using linear Palmgren–Miner model, Hashin and Rotem model and the residual strength degradation model are 44%, 42% and 25%, respectively. In order to compare them visually, experimental and numerical results of fatigue lives under block loading are plotted in Figure 10. It can be seen from Table 3 and Figure 10 that the residual strength degradation-based model provides more accurate fatigue life prediction than the linear and nonlinear Miner models. It is similar to the results for edge notched composite laminates in Wan et al.[34] that the maximum relative deviations between experimental results and life predictions by Palmgren–Miner rule and residual strength model are 43% and 30%. Considering the large scatter of fatigue data of composite materials, the relative deviation of 25% could represent a good accuracy of fatigue life prediction, which is consistent with the statements in Bendouba et al.[20] and Schaff and Davidson.[24] Bendouba et al.[20] evaluated the fatigue life of carbon/epoxy composite laminates under two-stage (low–high and high–low) block loading by using linear Palmgren–Miner and proposed nonlinear Miner model. It was found that the maximum relative deviations between numerical predictions and experiments for linear and nonlinear Miner are 1300% and 28%, respectively, indicating that the proposed nonlinear Miner model can predict fatigue life well. Schaff and Davidson[24] developed a residual strength model for fatigue life prediction of graphite/epoxy composite laminates under randomly ordered spectrum loading that has a maximum relative deviation of 32% to test results, showing good correlation between life predictions and experiments.

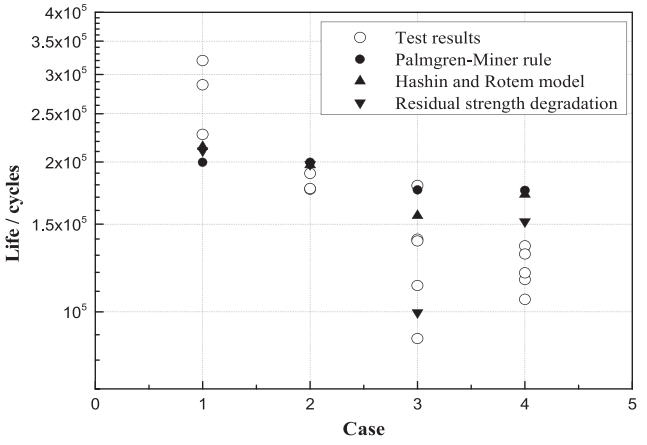


**FIGURE 10** Comparison between life predictions and experimental results under block loading (Case 1: graphite fibre-reinforced polymer [GFRP] under high–low sequence, Case 2: GFRP under low–high sequence, Case 3: GFRP under high–low–high sequence, Case 4: carbon fibre-reinforced polymer under high–low–high sequence)

## 4 | DISCUSSION

The validity of the modified residual strength model for fatigue life prediction of woven composite laminates has been demonstrated against the test results in Section 4. Good agreement has been achieved between fatigue life predictions and experiments for woven GFRP and CFRP composites with 8-mm initial delamination under tension–tension and compression–compression loading. The residual strength degradation-based model provides more accurate fatigue life prediction than the traditional linear damage accumulation models under block loading, which is attributed to the capacity of the model to consider the loading sequence effect. It is expected that the improvement in life prediction accuracy with the residual strength degradation-based model will be significantly greater when the difference in stress levels between the low block and the high block increases.

Figure 11 shows the different strength degradation behaviour plotted with the $s - n - R$ fatigue surface models for woven GFRP composites with 8-mm initial delamination under low–high and high–low sequence. There is an interaction between the two load blocks, and the interaction is significantly affected by the sequence of

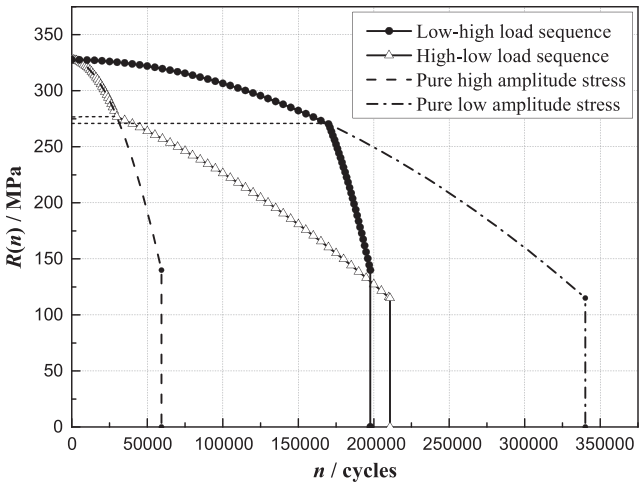


**FIGURE 11** Strength degradation of woven graphite fibre-reinforced polymer composites under low–high and high–low sequence

load blocks. The fatigue life is predicted by the residual strength degradation-based model with the criterion that fatigue failure happens when the maximum fatigue stress is equal to the residual strength. This makes the allowable total strength degradation (or damage accumulation) dependent on the maximum fatigue stress of the final fatigue cycle. As shown in Figure 11, the allowable strength degradation (or damage accumulation) under pure low amplitude fatigue stress will be greater than that under pure high amplitude fatigue stress. The load sequence effect is hence introduced under block loading as the strength degradation (or damage accumulation) caused by first load block will influence the strength degradation at the second load block. Under low–high sequence in the current study, the low block consumes 50% of the fatigue life corresponding to the pure low amplitude fatigue stress. The corresponding residual strength degradation (or damage accumulation) to this 50% fatigue life consumption under the pure low amplitude fatigue stress is however greater than the residual strength degradation (or damage accumulation) corresponding to 50% fatigue life consumption under pure high amplitude fatigue stress. This means that more than 50% of the fatigue life, corresponding to the pure high amplitude fatigue stress, has been consumed at the beginning of the high block of the low–high sequence. As a result, the fatigue life of the high block of the low–high sequence will be shortened, causing the total fatigue life of the low–high sequence to be smaller than the prediction without considering load sequence effect. Same argument applies to explain the load sequence effect on fatigue life of the laminate under high–low sequence, making the total fatigue life of the high–low sequence greater than the prediction without considering load sequence effect.

The load sequence effect on fatigue life captured by the residual strength degradation-based model agrees with the experimental results of woven GFRP and CFRP composites with 8-mm initial delamination under block fatigue load. The fatigue damage accumulation at the first block of two-stage fatigue loading has influence on that at the following block, resulting in shorter fatigue life under low–high sequence than that under high–low sequence. The fatigue cycles at first stage of low–high sequence leads to a large amount of matrix cracking, which coalesces and triggers delaminations, disrupting the load transfer among the layers. Thus, a larger number of fibre breakage happens at the following high load stage, resulting in faster failure of the material. The total fatigue life of the material under low–high sequence is shorter than the prediction without considering loading sequence effect, which agrees with the prediction of the residual strength degradation-based model. On the other hand, the total fatigue life of the material under high–low sequence is longer than the prediction without considering load sequence effect. A possible explanation for this is that the fatigue cycles at the first stage of high–low sequence improve the alignment of the fibres, increasing the stress taken by the fibres at the following stage. It reduces the occurrence of matrix cracking and subsequent delamination at the second low load stage, retarding the final failure of the material.

It should be noted that the developed residual strength model is a phenomenological approach for predicting the fatigue life and residual strength of composite laminates with initial delamination damage, which has been shown to be effective for woven composite laminates considering the complexity in the damage modes and their interactions associated with the interlacing and undulating fibre tows. Future work is required to further develop the model by introducing the mesoscale geometrical details (such as fibre waviness), effect of stress relaxation on residual strength and mesomechanics. Experimental data of residual strength after fatigue and variable amplitude fatigue life of composite laminates with initial delamination are scarce and highly desirable. More experimental data of woven composite laminates with different delamination shapes and locations should be generated and used for the sensitivity study to improve the proposed residual strength model further.

## 5 | CONCLUSIONS

This research aims to develop an engineering tool to predict the residual service life of woven composite laminates with an initial delamination. Experimental and numerical study were conducted on delaminated woven GFRP and CFRP composites under static, constant amplitude fatigue and variable amplitude fatigue loading. Four conclusions are drawn as follows:

- A $s - n - R - k - r$ residual strength model accounting for the effects of normalized delamination size and stress ratio has been proposed for predicting residual strength and fatigue life of woven composites with initial delamination, showing good agreement with experiments.
- The life prediction based on Palmgren–Miner's linear damage accumulation model is not capable of accounting for loading sequence effect and thus remains questionable for predicting the fatigue life under variable amplitude loading. The residual strength degradation-based model can effectively consider the loading sequence effect and predict the variable amplitude fatigue life more accurately.

- A clear loading sequence effect exists in fatigue damage accumulation of woven GFRP and CFRP composites. The fatigue life under low–high sequence is shorter than that under high–low sequence. The repetitive changes between tensile and compressive fatigue cycles can significantly reduce the lives of woven composites.
- The phenomenological approach adopted in the current study in deriving the modified residual strength model proves to be effective in predicting key engineering parameter such as the residual service life of a complex system with multiple influential factors. It is expected that the same procedure can be applied to derive fatigue life prediction models for other complex material systems.

## ACKNOWLEDGEMENT

This project was supported by the National Natural Science Foundation of China (51375033 and 51875021).

## CONFLICT OF INTEREST

None.

## NOMENCLATURE

| | |
|---|---|
| b | Parameter of the residual strength model |
| C | Parameter of the residual strength model |
| CFRP | Carbon fibre reinforced polymer |
| d | Initial delamination size |
| $D_i$ | Cumulative damage index for the $i^{th}$ load block |
| GFRP | Glass fibre reinforced polymer |
| k | Initial delamination size normalized with the specimen width |
| m | Parameter of the residual strength model |
| n, N | Number of fatigue cycles |
| $n_i$ | Number of loading cycles of the $i^{th}$ load block |
| $N_i$ | Constant amplitude fatigue life at the stress level of the $i^{th}$ load block |
| $\Delta n$ | Increment of fatigue cycles |
| r | Stress ratio of a fatigue cycle |
| $r_0$ | Stress ratio for a specific fatigue cycle |
| $R_0$ | Static strength of the composite material with an initial delamination |
| $R_0^0$ | Static strength of the pristine composite material |
| $R^2$ | Square of the correlation coefficient |
| R(n) | Residual strength of the material after n number of fatigue cycles |
| s | Absolute maximum stress of a fatigue stress cycle |
| $S_{-1}$ | Fatigue endurance limit under fully reversed cyclic loading |
| $S_a$ | Stress amplitude of a fatigue cycle |
| $S_m$ | Mean stress of a fatigue cycle |
| $S_{max,r}$ | Maximum fatigue stress at the stress ratio of r |
| $S_{min,r}$ | Minimum fatigue stress at the stress ratio of r |
| $S_0$ | Fatigue strength of the composite material with an initial delamination |
| $S_0^0$ | Fatigue strength of the pristine composite material |
| W | Width of the specimen |
| $\alpha_1$ | Parameter of the modified residual strength model |
| $\alpha_2$ | Parameter of the modified residual strength model |
| $\beta_1$ | Parameter of the modified residual strength model |
| $\beta_2$ | Parameter of the modified residual strength model |
| $\sigma_b$ | Ultimate strength of the material |
| $\sigma_c$ | Compressive strength of the material |
| $\sigma_t$ | Tensile strength of the material |

## ORCID

*Junjiang Xiong* https://orcid.org/0000-0003-2979-4134
*Yigeng Xu* https://orcid.org/0000-0002-7194-2308

## REFERENCES

1. Angioni SL, Meo M, Foreman A. A comparison of homogenization methods for 2-D woven composites. *Compos Part B Eng*. 2011;42(2):181-189.
2. Wang XW, Pont-Lezica I, Harris JM, Guild FJ, Pavier MJ. Compressive failure of composite laminates containing multiple delaminations. *Compos Sci Technol*. 2005;65(2):191-200.
3. Grasso M, Xu YG, Ramji A, et al. Low-velocity impact behaviour of woven laminate plates with fire retardant resin. *Compos Part B Eng*. 2019;171:1-8.
4. Butler S, Gurvich M, Ghoshal A, et al. Effect of embedded sensors on interlaminar damage in composite structures. *J Intell Mater Syst Struct*. 2011;22(16):1857-1868.
5. Aslan Z, Daricik F. Effects of multiple delaminations on the compressive, tensile, flexural, and buckling behaviour of E-glass/epoxy composites. *Compos Part B Eng*. 2016;100:186-196.
6. Naik NK, Ramasimha R. Estimation of compressive strength of delaminated composites. *Compos Struct*. 2001;52(2):199-204.
7. Fu HM, Zhang YB. On the distribution of delamination in composite structures and compressive strength prediction for laminates with embedded delaminations. *Appl Compos Mater*. 2011;18(3):253-269.
8. Li HH, Yao YT, Guo LY, Zhang QH, Wang B. The effects of delamination deficiencies on compressive mechanical properties of reinforced composite skin structures. *Compos Part B Eng*. 2018;155:138-147.
9. Zhao LB, Liu YL, Hong HM, Wang KK, Zhao J. Compressive failure analysis for low length-width ratio composite laminates with embedded delamination. *Compos Commun*. 2018;9:17-21.
10. Davidson P, Waas AM. The effects of defects on the compressive response of thick carbon composites: an experimental and computational study. *Compos Struct*. 2017;176:582-596.

11. Davila CG, Bisagni C. Fatigue life and damage tolerance of post-tbuckled composite stiffened structures with initial delamination. *Compos Struct*. 2017;161:73-84.
12. Cruanes C, Shanwan A, Meo S, Deffargesa MP, Lacroixa F, Hivetb G. Effect of mesoscopic out-of-plane defect on the fatigue behavior of a GFRP. *Mech Mater*. 2018;117:214-224.
13. Colombo C, Vergani L. Influence of delamination on fatigue properties of a fibreglass composite. *Compos Struct*. 2014;107:325-333.
14. Lifshitz JM, Gildin D. Failure of delaminated carbon/epoxy composite beams under cyclic compression. *Compos Struct*. 1997;39(3-4):289-296.
15. Reis PNB, Ferreira JAM, Antunes FV, Richardson MOW. Effect of interlayer delamination on mechanical behavior of carbon/-epoxy laminates. *J Compos Mater*. 2009;43(22):2609-2621.
16. Liu H, Cui H, Wen W, Kang H. Fatigue characterization of T300/924 polymer composites with voids under tension–tension and compression–compression cyclic loading. *Fatigue Fract Eng Mater Struct*. 2018;41(3):597-610.
17. Behera A, Dupare P, Thawre MM, Ballal AR. Effect of fatigue loading on stiffness degradation, energy dissipation, and matrix cracking damage of CFRP [±45] 3S composite laminate. *Fatigue Fract Eng Mater Struct*. 2019;42(4):2302-2314.
18. Bond IP. Fatigue life prediction for GRP subjected to variable amplitude loading. *Compos A: Appl Sci Manuf*. 1999;30(8):961-970.
19. Philippidis TP, Vassilopoulos AP. Life prediction methodology for GFRP laminates under spectrum loading. *Compos A: Appl Sci Manuf*. 2004;35(6):657-666.
20. Bendouba M, Aid A, Benguediab M. Fatigue life prediction of composite under two block loading. *Eng Technol Appl Sci Res*. 2014;4:587-590.
21. Epaarachchi JA. A study on estimation of damage accumulation of glass fibre reinforce plastic (GFRP) composites under a block loading situation. *Compos Struct*. 2006;75(1-4):88-92.
22. Sarfaraz R, Vassilopoulos AP, Keller T. Block loading fatigue of adhesively bonded pultruded GFRP joints. *Int J Fatigue*. 2013;49:40-49.
23. Philippidis TP, Passipoularidis VA. Residual strength after fatigue in composites: theory vs. experiment. *Int J Fatigue*. 2007;29:2104-2116.
24. Schaff JR, Davidson BD. Life prediction methodology for composite structures. Part II—spectrum. *Fatigue J Compos Mater*. 1997;31(2):158-181.
25. Hosoi A, Kawada H, Yoshino H. Fatigue characteristics of quasi-isotropic CFRP laminates subjected to variable amplitude cyclic two-stage loading. *Int J Fatigue*. 2006;28(10):1284-1289.
26. Passipoularidis VA, Philippidis TP. A study of factors affecting life prediction of composites under spectrum loading. *Int J Fatigue*. 2009;31(3):408-417.
27. Post NL, Case SW, Lesko JJ. Modeling the variable amplitude fatigue of composite materials: a review and evaluation of the state of the art for spectrum loading. *Int J Fatigue*. 2008;30(12):2064-2086.
28. Broutman LJ, Sahu S. A new theory to predict cumulative fatigue damage in fiberglass reinforced plastics. Composite materials: Testing and design (second conference). ASTM International, 1972.
29. Kassapoglou C. Fatigue of composite materials under spectrum loading. *Compos A: Appl Sci Manuf*. 2010;41(5):663-669.
30. Eskandari H, Kim HS. A theory for mathematical framework of fatigue damage on SN plane. *Key Eng Mater*. 2015;627:117-120.
31. Eskandari H, Kim HS. A theory for mathematical framework and fatigue damage function for the SN plane. Fatigue and Fracture Test Planning, Test Data Acquisitions and Analysis, ASTM STP1598; 2017: 299–336.
32. Guedes RM. Novel analytical model for fatigue cumulative damage estimation under random loading. *Fatigue Fract Eng Mater Struct*. 2019;42(8):1662-1678.
33. Xiong JJ, Shenoi RA. Two new practical models for estimating reliability-based fatigue strength of composites. *J Compos Mater*. 2004;38(14):1187-1209.
34. Wan AS, Xu YG, Xiong JJ. Notch effect on strength and fatigue life of woven composite laminates. *Int J Fatigue*. 2019;127:275-290.
35. ASTM D5766-11. Standard test method for open-hole tensile strength of polymer matrix composite laminates; 2011.
36. ASTM D6484-09. Standard test method for open-hole compressive strength of polymer matrix composite laminates; 2009.
37. Xiong JJ, Shenoi RA. A two-stage theory on fatigue damage and life prediction of composites. *Compos Sci Technol*. 2004;64(9):1331-1343.
38. Xiong JJ, Shenoi RA. *Fatigue and Fracture Reliability Engineering*. London: Springer; 2011.
39. Hashin Z, Rotom A. A cumulative damage theory of fatigue failure. *Mater Sci Eng A*. 1978;34(2):147-160.


**How to cite this article:** Wan A, Xiong J, Xu Y. Fatigue life prediction of woven composite laminates with initial delamination. *Fatigue Fract Eng Mater Struct*. 2020;43:2130–2146. https://doi.org/10.1111/ffe.13296